



ELSEVIER

Marine Geology 186 (2002) 423–446



www.elsevier.com/locate/margeo

The origin and preservation of a major hurricane event bed in the northern Gulf of Mexico: Hurricane Camille, 1969

Samuel J. Bentley^{a,*}, Timothy R. Keen^b, Cheryl Ann Blain^b,
W. Chad Vaughan^c

^a *Department of Oceanography and Coastal Sciences, and Coastal Studies Institute, Louisiana State University, Baton Rouge, LA 70803, USA*

^b *Naval Research Laboratory, Oceanography Division, Stennis Space Center, MS 39529, USA*

^c *Naval Research Laboratory, Seafloor Sciences Division, Stennis Space Center, MS 39529, USA*

Received 23 May 2001; accepted 5 April 2002

Abstract

Cores collected from Mississippi Sound, in the Gulf of Mexico, were studied using $^{210}\text{Pb}_{\text{xs}}$ and ^{137}Cs geochronology, X-radiography, granulometry, and a multi-sensor core logger. Our results indicate the presence of a widespread sandy event layer that we attribute to Hurricane Camille (1969). An initial thickness of more than 10 cm is estimated from the cores, which is large compared to the time-averaged apparent accumulation rate of 0.29–0.47 cm y^{-1} . Physical and biological post-depositional processes have reworked the sandy layer, producing a regional discontinuity and localized truncation, and resulting in an imperfect and biased record of sedimentary processes during the storm. The oceanographic and sedimentological processes that would have produced an event bed during Hurricane Camille are simulated using a series of numerical models, i.e. (1) a parametric cyclone wind model, (2) the SWAN third-generation wave model, (3) the ADCIRC 2D finite-element hydrodynamic model, and (4) a wave-current bottom boundary layer model that is coupled to transport and bed conservation equations (TRANS98). The simulated bed ranges from 5 cm to over 100 cm within a tidal channel near the barrier islands. Seaward of the islands, the bed is more than 10 cm in thickness with local variability. The magnitude and local variability of the storm bed thickness are consistent with the observed stratigraphy and geochronology on both the landward and seaward sides of the barriers. © 2002 Elsevier Science B.V. All rights reserved.

Keywords: hurricanes; event beds; geochronology; numerical models

1. Introduction

Both modern and ancient continental shelf strata frequently consist of hummocky cross-stratified

sand or sandstone layers intercalated with mud or shale. The sandy beds are called event beds because their erosive bases and sedimentary and biogenic structures indicate that they were emplaced by flows at the event scale (Seilacher, 1982), on the order of a few hours or days duration. Storms have been shown to be the mechanism for formation of these beds on modern shelves (Hayes, 1967; Swift et al., 1981; Morton, 1981; Nelson,

* Corresponding author. Tel.: +1-225-578-2954; Fax +1-225-578-2520.

E-mail addresses: sjb@lsu.edu (S.J. Bentley), keen@nrlssc.navy.mil (T.R. Keen).

1982; Snedden et al., 1988; Figueiredo et al., 1982; Gagan et al., 1990), and have been suggested as the origin of sandstone event beds (Brenchley et al., 1986; Snedden and Nummedal, 1990; Swift et al., 1987).

Our present understanding of storm sedimentation is contained within the models of Dott and Bourgeois (1982), Walker (1984), Brenchley (1985), Duke (1985), Duke et al. (1991), and Swift and Thorne (1991). While representing an important conceptual advance, these models are primarily qualitative. They do not make testable predictions of the distribution of storm beds in modern environments. Sedimentary strata predicted by geologically relevant models like that of Thorne et al. (1991) are quantitative and can thus be compared to ancient sequences, but they do not make predictions about individual beds, which can be tested against modern oceanographic data. The quantitative characteristics of individual storm beds can be simulated by a physics-based numerical model like the one used to examine event bed genesis in the Gulf of Mexico (Keen and Slingerland, 1993a,b; Keen and Glenn, 1998), the Middle Atlantic Bight of North America (Keen and Glenn, 1994a), the East China Sea (Flaum et al., 2000), and the Cretaceous Western Interior Seaway of North America (Slingerland and Keen, 1999).

The observations needed to evaluate the event layers predicted by single-bed models like that of Keen and Slingerland (1993a) have been scarce in the past because of problems of scale and the preservation of these thin sand beds. Snedden et al. (1988) and Morton (1981) have described the spatial extent of event beds deposited on the Texas coast during hurricanes but definitive evidence of the correlation of these beds was lacking because of reworking of the bed. In order to identify an individual storm bed in multiple cores with sufficient accuracy to test the quantitative predictions of a numerical model, it is necessary to have better control on the time of deposition of possible beds. It is also important that bed amalgamation and reworking are minimal.

Hurricane Camille was the second strongest hurricane to hit the U.S. coastline in the twentieth century. The eye made landfall at Waveland, MS

(Fig. 1) at 04.30 h UT on August 17, 1969. The central pressure was 901 mb and the maximum sustained winds near the eye were more than 85 m s^{-1} just before landfall (Neumann, 1993). The storm surge within Mississippi Sound exceeded 7 m. Bottom currents on the Florida coast 150 km east of landfall were measured at more than 1.6 m s^{-1} (Murray, 1970). Prior to Camille, there were no major hurricane strikes along this coast since 1947. Between 1969 and 2000, the only hurricanes to make landfall on the Mississippi coast were Elena (1985, storm surge 2.6 m, Biloxi, MS), and Georges (1998, storm surge ~ 2 m, Ocean Springs, MS) (Neumann, 1993; Stone et al., 1999). No studies of the impacts of Hurricane Elena on the seabed of Mississippi Sound or the adjacent continental shelf have been published. Both Elena and Georges were much weaker than Camille and cores collected in Mississippi Sound several months after Georges did not contain a significant preserved event layer (S.J. Bentley, unpublished data). Thus, Georges is not expected to have had a widespread effect on the amalgamation of previous storm beds, and the effects of Elena, although possibly significant, are likely to have been much less than those of Camille. It seems probable that if an identifiable and datable event bed is to be found anywhere in the U.S. coastal waters, it may well be in the sheltered waters of Mississippi Sound, and it may have been deposited by Hurricane Camille in 1969.

The objectives of this paper are: (1) to determine the degree of preservation and characteristics of a sandy layer that we propose was deposited by Hurricane Camille as it made landfall in the northern Gulf of Mexico, and (2) to use a numerical model to conceptualize the relationships between the physical forcing and the initial extent and thickness of the event bed deposited by Hurricane Camille. We will show by means of sedimentological and radiochemical analyses that numerous cores from Mississippi Sound and the adjacent shelf contain a sandy layer that was probably deposited by Hurricane Camille. This study also makes quantitative predictions of sediment resuspension and transport within Mississippi Sound during Hurricane Camille and uses them

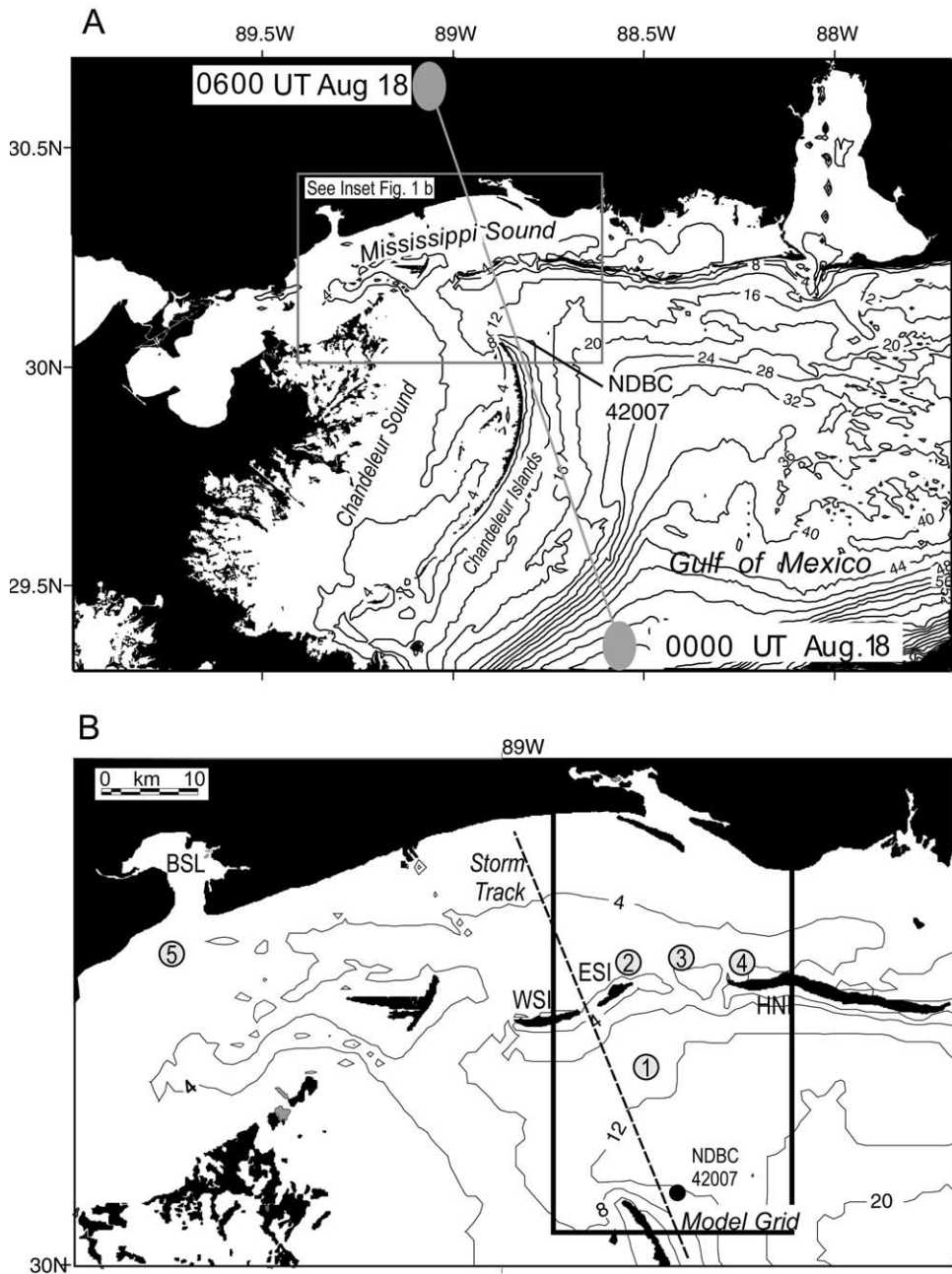


Fig. 1. (A) Map of the Mississippi Bight study area. Large black dots mark the position of Hurricane Camille as it made landfall on August 18, 1969. Location of National Data Buoy Center (NDBC) Station 42007 is indicated close to the storm track. (B) The highlighted rectangle is the grid used for the sedimentation model. Abbreviations of barrier islands: HNI, Horn Island; ESI, East Ship Island; WSI, West Ship Island; CNI, Chandeleur Islands; other abbreviation: BSL, Bay St. Louis. The numbers refer to locations where the cores listed in Table 1 were collected. Water depth is indicated in meters.

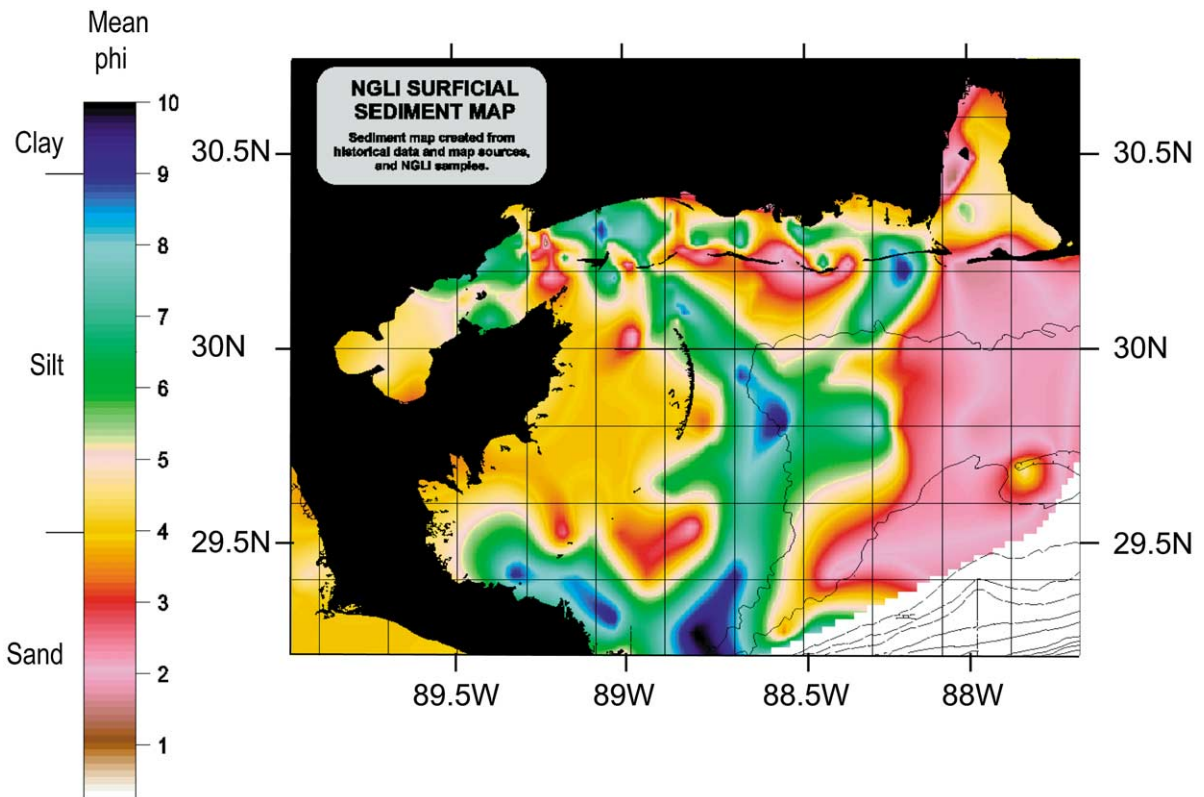


Fig. 2. Map of bottom sediment mean grain size in ϕ units in Mississippi Bight, from Sawyer (2001).

to evaluate the initial characteristics of the Camille event bed. Comparison of the analytical and numerical results thus improves our understanding of event bed deposition and post-depositional modification in coastal areas.

2. Study area

The south-facing barrier islands fronting Mississippi Sound (Fig. 1) formed by upward aggradation, as longshore currents transported sediment from Mobile Bay westward (Otvos, 1970, 1979). Sediment within Mississippi Sound (Fig. 2) consists of medium to coarse sand along the barrier islands and silt and clay located within the central parts (Upshaw et al., 1966; Sawyer, 2001). Overall, the northern Gulf barrier islands are migrating to the west in response to wave-

driven longshore drift (Stone and Stapor, 1996). West Ship Island has recently slowed its migration because of dredging in the ship channel to the west. Ship Island, consisting of West Ship Island and East Ship Island, now appears to be rotating counterclockwise as East Ship Island is eroding on its Gulf side. The rotation is partly attributed to accretion on the Gulf coast of West Ship Island while erosion is occurring on its sound side.

The Chandeleur Islands are a curved east-facing barrier chain fronting Chandeleur Sound. The sediments of Chandeleur Sound comprise clay, silt and sand. The dominant geomorphic factors in the evolution of the Chandeleur barrier island chain are tropical cyclones, which commonly overwash these low-lying islands and incise channels through them (Kahn and Roberts, 1982). Hurricane Frederick (1979) flattened the dunes of the southern Chandeleur Islands and they re-

main a shoal today because of more recent storms such as Hurricane Georges, 1998 (Stone and Wang, 1999).

3. Methods

3.1. Core retrieval and analysis

During cruises on the R/V *Kit Jones* between July 1999 and May 2001, box cores and gravity cores (Table 1) were collected in western and central Mississippi Sound and the adjacent inner shelf in water depths between 4 and 10 m (see Fig. 2 for locations). Sampling locations were placed in muddy seabed near the mud–sand transition both seaward and landward of the barrier islands. The sampling locations were based on the hypothesis that if event layers were preserved, identification would be facilitated by lithologic contrast between sandy event beds and muddy matrix. Differential GPS was used for positioning, allowing precise reoccupation of stations on multiple cruises. Only undisturbed cores with no evidence of slumping or surface distortion were retained for subsampling. Box cores were subsampled for radioisotopes and physical properties using 10-cm-internal-diameter PVC pipe that was inserted into the sediment, withdrawn, and extruded at 1–2 cm intervals for analysis. Slabs for X-radiography were obtained by pushing open-ended, three-sided Plexiglas trays (2.5 cm thick \times 16 cm wide) into core boxes on deck, then inserting the fourth side so as to minimize fabric distortion. On the day of collection, slabs were X-radiographed using a portable veterinary

X-ray unit. X-ray negatives were then digitized for image analysis.

Gravity cores were analyzed using a GEOTEK Multi-Sensor Core Logger (MSCL), an automated system in which cores are logged horizontally. An ultrasonic P-wave system measured P-wave speed through the cores at 500 kHz. Gamma ray density (attenuation) was measured from a narrow beam of gamma rays emitted from a 10 milli-curie ^{137}Cs source with energies principally at 661 KeV. Measurements were conducted at atmospheric pressure, with cores equilibrated to laboratory ambient temperature (23°C). Subsamples were also retained for radioisotope and granulometric analysis.

Cores analyzed for sand content were collected on different dates but from the same stations as the cores analyzed by X-radiography, radiochemistry, and MSCL. Patterns of grain size were assessed by measuring percent sand and mud in samples that were dispersed in 0.05% sodium metaphosphate solution, disaggregated in an ultrasonic bath, then wet-sieved at 4 ϕ (63 μm). Mud and sand fractions were dried and weighed. Masses were corrected for interstitial salts and dispersant.

Activities of ^{210}Pb (natural product of U-series decay; $t_{1/2} = 22$ yr) and ^{137}Cs (product of nuclear fission in nuclear reactors and bombs, $t_{1/2} = 30.7$ yr) were determined by γ -spectroscopy analysis of dried sediment (46.5 KeV peak for ^{210}Pb and 661 KeV peak for ^{137}Cs). ^{210}Pb activities were corrected for self-absorption by calibration with standards of known activity (Cutshall et al., 1983). Excess activities of ^{210}Pb ($^{210}\text{Pb}_{\text{xs}}$) were determined by comparison with supported activities

Table 1
Summary of cores and stations discussed in this paper

Station Number On Fig. 1	Station name	Box cores	Gravity cores
1	Inner shelf	KJ070600 BC8	KJ070600 GC8
2	East Ship Island	KJ070600 BC6	KJ070600 GC6
3	Dog Key Pass	KJ040500 E	none
4	Horn Island	KJ070600 BC1 KJ040500 D	KJ070600 GC1
5	Bay St. Louis	KJ 0501 D BSL070999 BCE KJ070999 BCE	BSL091399 GCA

of parent radionuclides ^{214}Pb (295 and 351 KeV) and ^{214}Bi (609 KeV). The minimum detection limit for ^{137}Cs was 0.05 decays per minute per gram (dpm g^{-1}) in 17-g samples. Activities for all radioisotopes are reported in dpm g^{-1} , with 60 dpm g^{-1} equivalent to 1 Bq g^{-1} .

3.2. Numerical methods

One approach to examine the physical processes that affect storm deposition within the Mississippi Bight during hurricanes is to use numerical wind, wave, and current models. The wind, wave, and current simulations were completed for 14–19 August 1969. The bottom topography used in the simulations comes from the National Ocean Service 3-sec database and local surveys made during the Northern Gulf of Mexico Littoral Initiative Project of the Naval Oceanographic Office.

A parametric cyclone wind model gives good results for areas within the radius of maximum winds (Keen and Slingerland, 1993a). The wind field for these simulations is computed on a 5-km grid of the entire Gulf of Mexico.

The steady currents are calculated by the ADCIRC-2DDI hydrodynamic model, the depth-integrated option of a set of two- and three-dimensional fully non-linear codes named ADCIRC (Leutlich et al., 1992). ADCIRC-2DDI solves the vertically integrated equations for mass and momentum conservation on a grid with linear, triangular finite elements. The model as used in this study does not include coastal flooding and drying. The model domain includes the entire Gulf of Mexico and the western North Atlantic, with resolution varying from 98 km in the open ocean to 500 m near tidal inlets (Blain, 1997). The astronomical tides are not calculated for this simulation because of their minimal impact during the hurricane. No river inflow is incorporated into the model.

It is not sufficient to compute only steady currents if sediment transport is to be calculated because sediment resuspension is dominated by waves in shallow water. Consequently, this study utilizes the third-generation spectral SWAN model (Simulating Waves Nearshore) (Booij et al., 1999; Ris et al., 1999) to compute waves. The

SWAN model calculates refraction, wave breaking, dissipation, wave-wave interaction, and local wind generation. The wave model grid is the same as the wind grid. The resulting low resolution within the Sound is considered reasonable for this study because highly detailed wave fields are not necessary and cannot be validated. The water depth used in SWAN changes with the water surface elevation and, therefore, larger storm waves can be computed in otherwise shallow water within the estuary. The wave model does not calculate waves over the islands when they are submerged, however.

The bottom boundary layer model (BBLM) of Glenn and Grant (1987) has been modified to promote better convergence of the numerical solution for a wider range of waves and currents (Keen and Glenn, 1994b). This enhanced model is coupled to a sediment transport and bed conservation model. The resulting coupled BBLM-sedimentation model, TRANS98 (Keen and Glenn, 1998), is used in this study. One advantage of this coupled model is that it computes the bed roughness in conjunction with the suspended sediment profiles. Furthermore, because of the coupling between the BBLM and the sedimentation-bed conservation model, changes in the bed properties and elevation due to resuspension, erosion, and deposition feed back to the BBLM.

Several wave, current, and sediment parameters must be given at each grid point in the domain. The significant wave height H_s , peak period T , and mean propagation direction θ of the wave field at each grid point are available from the SWAN wave simulation. The wave orbital speed u_b and diameter A_b are computed using linear wave theory. The reference currents u_r from ADCIRC are located at mid-water depth. The angle between the steady current and wave directions φ_r is also found. The choices of eddy diffusivity and resuspension coefficients used in calculating the suspended sediment profiles are based on a previous sensitivity study (Keen and Stavn, 2000).

Current and suspended sediment concentration profiles are computed every time step. The physical bottom roughness k_b is calculated by the BBLM as described by GG87 using the mean diameter of sediment in the bed at each grid point.

The BBLM explicitly includes bed armoring as finer material is preferentially removed because the remaining bed sediment is coarser. The depth of entrainment is restricted by the active layer h_A , which represents that part of the bed that interacts with the flow during one time step. When low flow conditions exceed the initiation of motion criteria, the active layer is assumed to be proportional to the ripple height (Grant and Madsen, 1982). During high flow conditions, it will be proportional to the height of the near-bed transport layer h_{TM} . The active layer height is given by $h_A = \eta + C \cdot h_{TM}$, where η is the ripple height and C is a proportionality constant for the average concentration in the near-bed transport layer. When the depth of resuspension for a sediment size class exceeds h_A at a grid point, the reference concentration is reduced and new profiles of currents, sediment concentrations, and stability parameters are calculated. This iterative procedure is applied at each grid point for each sediment size class.

Since the model as implemented in this study does not include overtopping of barrier islands or coastal areas by the storm surge, it is necessary to represent coastal erosion by introducing sediment at landward grid points. A no-gradient boundary condition is applied for transports at the coast and the open boundaries of the model grid. This coastal erosion simulates erosion from the interior of the islands during overwash, as well as beach erosion. Thus, sediment is input to the model grid wherever erosion is predicted at wet points adjacent to land. This boundary condition assumes that landward erosion by waves or overtopping is adequate to supply a sufficient sediment volume to the shallowest wet grid point to prevent erosion. This treatment is necessary because the model does not calculate sediment entrainment by breaking waves. A similar boundary condition is included at open boundaries, except that sediment can leave the model grid as well as enter it.

The numerical sedimentation model is being used in this study to evaluate the relationships between the waves and currents and the initial Camille sand bed within the Mississippi Sound region. Thus, it is important for the model to incorporate several processes that control sedi-

mentation such as bed armoring, wave–current interaction, and advection by steady flows. An assumption in this approach is that sand and silt resuspension and transport during the hurricane is independent of cohesive sediment transport. This approach also implies that the entrainment of sand will be the limiting factor in resuspension. Although this is clearly not the case when the sand concentration is low, it is a reasonable first approximation because of the lack of quantitative data on the entrainment rates for mixed (sand–silt–clay) sediments. This assumption is justified during deposition of the storm bed because mud remains in the water column much longer than coarser sediment. Consequently, a sand layer will be deposited independently of cohesive sediment. This study examines this sand layer only. The non-cohesive sediment component is represented by ten size classes of silt and sand, with a mean of 0.088 mm (3.5 ϕ). More realistic sediment distributions are available (Fig. 2) but are not used in order to simplify interpreting the model results. The sedimentation model uses a grid with a horizontal resolution of approximately 650 m and 31 vertical levels.

4. Core analysis results

4.1. Radioisotope geochronology

Core profiles of $^{210}\text{Pb}_{\text{xs}}$ (Fig. 3) show significant variability between stations, with some shared attributes. Individual profiles are irregular, lacking the gradual exponential decay with increasing depth that is associated with steady-state processes of sediment bioturbation and accumulation (for example, Nittrouer and Sternberg, 1981; Bentley and Nittrouer, 1999). Gradients in the uppermost 5–10 cm of all profiles vary widely. Nearly zero gradients in this zone are probably attributable to a combination of both biological and physical mixing, based on fabric evidence (Fig. 5) of bioturbation and stratification; for example, faint bedding in the upper 5 cm at Horn Island (core KJ070600 BC1) and bedding at approximately 7 cm on the inner shelf (core KJ070600 BC8). Numerous macrobenthos that were observed dur-

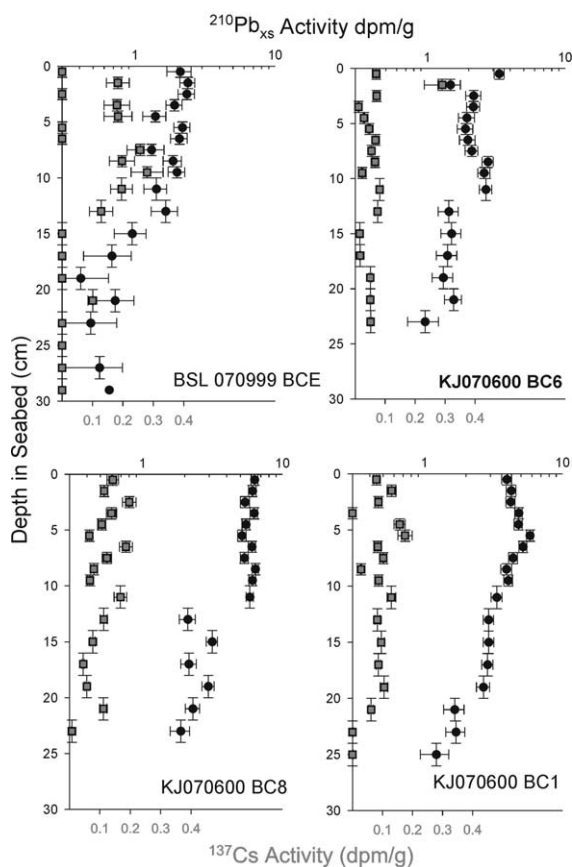


Fig. 3. Profiles of $^{210}\text{Pb}_{\text{xs}}$ (circles) and ^{137}Cs (squares) from boxcores in the study area, near Bay St. Louis (BSL070999 BCE), East Ship Island (KJ070600 BC6), Horn Island (KJ070600 BC1), and the adjacent inner continental shelf (KJ070600 BC8). For each core, note the similar discontinuities in $^{210}\text{Pb}_{\text{xs}}$ profiles at ~ 12 cm bsf, and the similar penetration depth of ^{137}Cs (20–22 cm). The discontinuities are indicative of non-steady state deposition and/or mixing.

ing core subsampling are also indicative of bioturbation. Mixing processes, whether physical (Dellapenna et al., 1998) or biological (e.g. Beninger et al., 1979), tend to homogenize particle-bound radioisotopes as well as sediment, resulting in a reduced gradient of radioisotope activity with depth. A recent seabed study of Mississippi Sound

(Bentley et al., 2000) observed that rapid bioturbation is limited to the upper 5–7 cm, consistent with the $^{210}\text{Pb}_{\text{xs}}$ profiles shown here.

A trait common to all of the $^{210}\text{Pb}_{\text{xs}}$ profiles shown in Fig. 3 is the presence of a vertical zone of nearly constant (or low but variable) activity ranging from approximately 12 to the maximum depth of each core (~ 25 cm). The upper boundary of this zone varies from being a sharp discontinuity at East Ship Island (core KJ070600 BC6) to a change in gradient with no sharp discontinuity at Horn Island (core KJ070600 BC1). Surface activities are lowest (3–5 dpm g^{-1}) for inshore cores, and highest (approximately 7 dpm g^{-1}) for the inner shelf (core KJ070600 BC8). This is presumably associated with increasing $^{210}\text{Pb}_{\text{xs}}$ water-column inventories in higher-salinity bottom water beyond the estuarine Mississippi Sound (e.g. Cochran, 1982).

Apparent sediment-accumulation rates (s , cm y^{-1}) were calculated for $^{210}\text{Pb}_{\text{xs}}$ profiles below the estimated depth of bioturbation using a least-squares fit of the following equation to the $^{210}\text{Pb}_{\text{xs}}$ profiles:

$$A(z) = A_0 \exp\left(\frac{-\lambda z}{s}\right) \quad (1)$$

where λ is the decay constant for the radionuclide of interest (0.031 y^{-1} for ^{210}Pb) and A is excess activity (dpm g^{-1}) at depth z (Nittrouer and Sternberg, 1981; Table 2). This approach assumes steady-state sediment accumulation, constant $^{210}\text{Pb}_{\text{xs}}$ activity at $z=0$, and no bioturbation effects on the portion of the $^{210}\text{Pb}_{\text{xs}}$ profile for which the least-squares fit is conducted. It is unlikely that these conditions are met for the cores shown in Fig. 3 but the approach does provide a simple means for comparing profile shape. It also provides an estimate of the *maximum possible* sediment accumulation rate over the past 50 yr (approximately two half lives of ^{210}Pb), based on

Fig. 4. X-radiographic negatives of box cores from the study area. Bright zones correspond to zones with high bulk density (sand) and dark zones correspond to low bulk density (mud). For comparison with radionuclide profiles, depth to disturbed portion of $^{210}\text{Pb}_{\text{xs}}$ profiles and maximum penetration depth of ^{137}Cs is indicated.

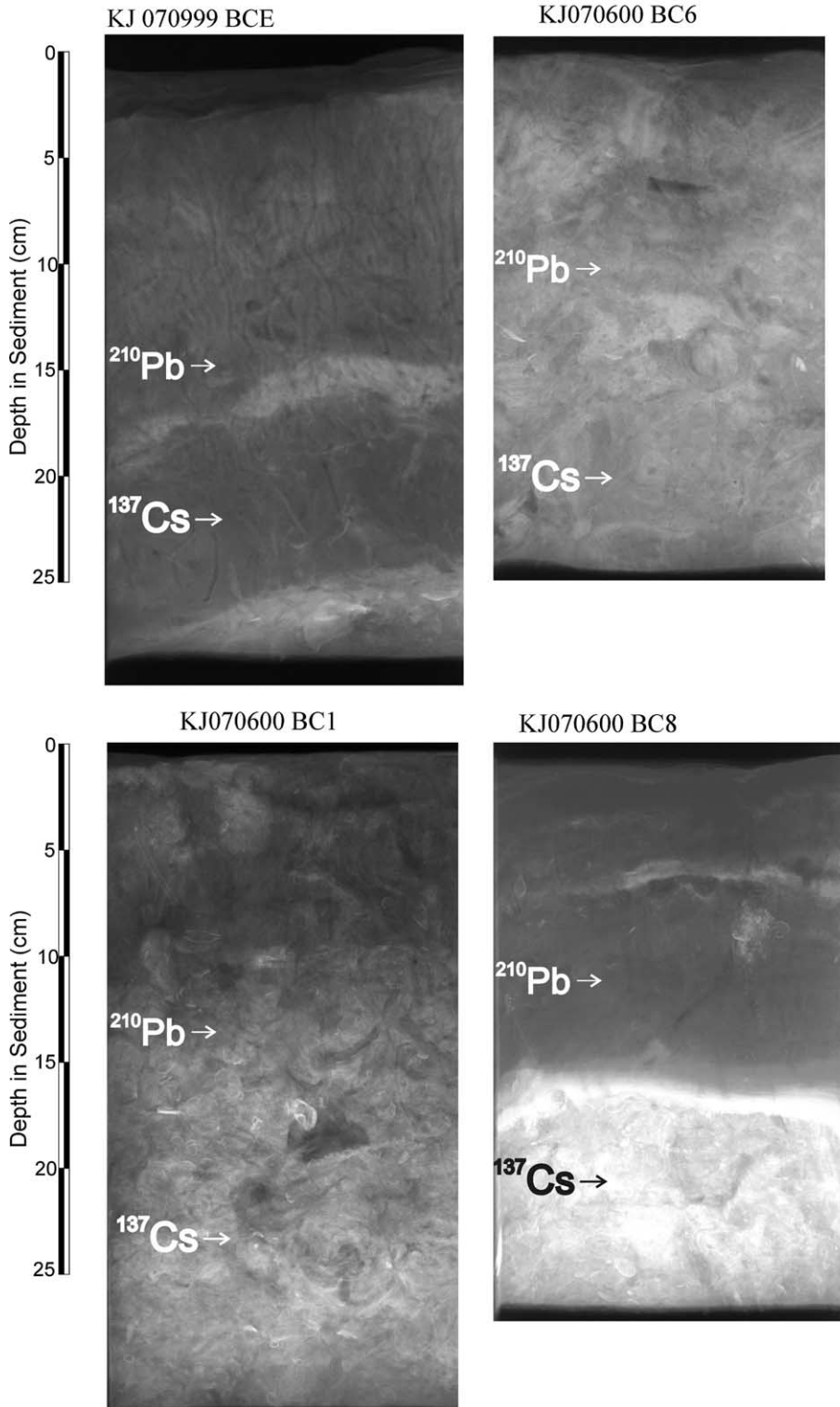


Table 2
Characteristics of ^{210}Pb profiles in Fig. 3

Profile parameter	BSL 070999BCE Bay St. Louis	KJ070600BC1 Horn Island	KJ070600BC6 East Ship Island	KJ070600BC8 Inner Shelf
S , cm y^{-1}	0.31	0.47	0.44	0.29
r^2	0.67	0.91	0.76	0.68
Depth range (cm)	13–27	5–24	8–24	8–24

Sediment accumulation rate, S , is calculated from results of least-squares fits of Eq. 1 (steady-state advection/decay model) to $^{210}\text{Pb}_{\text{xs}}$ profiles to estimate maximum rate sediment accumulation.

the activities at the top and bottom of the profiles in Fig. 3. This time-averaged rate is between 0.29 and 0.47 cm y^{-1} (Table 2).

^{137}Cs is an anthropogenic impulse tracer that was introduced into the environment in atmospheric atomic bomb testing starting in 1954. It reached a peak in 1963 and input has been declining ever since. ^{137}Cs usually adsorbs strongly and irreversibly to particle surfaces. Profiles of ^{137}Cs show low and variable activities to depths of approximately 22 cm in the central Mississippi Sound and the adjacent inner shelf, and 18–22 cm in the western Mississippi Sound, below which depths ^{137}Cs is not detectable. Because the seafloor in Mississippi Sound is probably influenced both by intense bioturbation and physical reworking during storms, it is not appropriate to use the maximum penetration depth of ^{137}Cs to directly calculate sediment accumulation rates (e.g. Nittrouer et al., 1984; Bentley and Nittrouer, 1999). However, the presence of ^{137}Cs at depths of 18–22 cm demonstrates that some portion of the sediment at that depth has been deposited since the 1954–1963 time frame, even if ^{137}Cs -labeled particles have been mixed downward by physical and biological processes.

4.2. X-radiography

Sedimentary fabric in X-radiographs (Fig. 4) ranges from partially stratified on the inner shelf (core KJ070500 BC8) and at Bay St. Louis (core KJ070999 BCE) to intensely bioturbated at East Ship Island (core KJ070600 BC6). All X-radiographs indicate sandy layers (bright zones) at depths of 10–15 cm below seafloor (bsf). The sharpest contacts are preserved on the inner shelf

(core KJ070600 BC8), where a layer of laminated sand with a distinct base at approximately 17 cm bsf overlies coarser shelly sediments. The less distinct layers may have resulted from intermixing of sand beds with muddier sediment. Biogenic fabric dominates at Horn Island (core KJ070600 BC1) and East Ship Island (core KJ070600 BC6), and mottling is produced by the density contrast between swirls of intercalated sandy and muddy sediment.

For comparison with the radionuclide profiles in Fig. 3, both the maximum penetration depth of ^{137}Cs and the depth of sharp breaks in profiles for each core are marked on the X-radiographs in Fig. 4. In general, the depth interval bounded by these two features in radionuclide profiles coincides in X-radiographs with sandy and sometimes physically stratified sediment in an otherwise muddy matrix. It is important to note that the observed $^{210}\text{Pb}_{\text{xs}}$ and ^{137}Cs reference depths do not correspond to lithologic boundaries, and, consequently, are not exclusive products of vertical changes in particle type or size.

4.3. Sand content

Sand concentration ranges between approximately 10 and 50% by mass in box cores from Bay St. Louis (Fig. 5A) and Horn Island (Fig. 5B) regions of Mississippi Sound. Subsurface maxima for sand content occur in the Horn Island core (KJ040500D) at about 17 cm bsf, near the center of the zone delineated by the $^{210}\text{Pb}_{\text{xs}}$ and ^{137}Cs reference depths (12 and 22 cm bsf, respectively, in KJ 070600 BC1; Fig. 3) in another core from the same station. Similarly, a subsurface sand maximum occurs in core KJ0501 D at

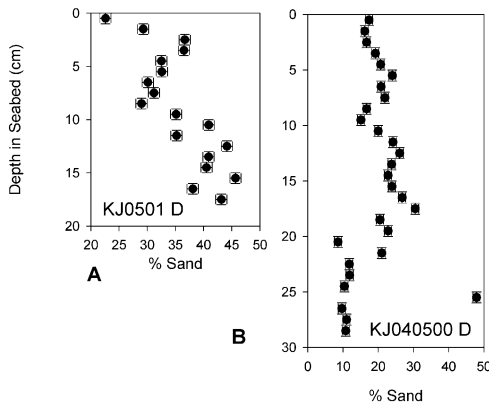


Fig. 5. Sand content of box cores from (A) Bay St. Louis and (B) Horn Island (Fig. 2; Table 1). Horizontal error bars indicate the standard deviation of three replicate measurements made for one depth interval in each core (~1%). Sub-surface maxima in both cores (15–17 cm bsf) correspond to basal zones in radiochemical profiles delineated by uniform ^{210}Pb activity and maximum depth of ^{137}Cs (Fig. 3), and to gamma-density maxima in corresponding gravity cores (Fig. 6).

~15 cm bsf, which corresponds closely to the $^{210}\text{Pb}_{\text{xs}}$ and ^{137}Cs reference depths in core BSL 070900 BCE (Fig. 3; collected from the same lo-

cation as KJ0501 D), and the depth of a sandy bed visible in the X-radiograph of BSL 070900 BCE (Fig. 4).

4.4. Logs of sound speed and bulk density

Maximum values for sound speed and gamma density (sediment bulk density determined from gamma-attenuation; Fig. 6) occur in each core between approximately 15 and 30 cm bsf. Compressional sound speed is a function of grain mineralogy, particle size, and bulk density as well as other parameters, and so correlates with bulk density and mineralogy (i.e. sand versus mud). At Bay St. Louis (core BSL091399 GCA), two distinct maxima are evident. The gamma density data on the inner shelf (core KJ070600 GC8) suggests the presence of sandy layers at 8–13 cm bsf and 17–29 cm bsf, separated by a muddy layer. More subtle subsurface gamma-density maxima are evident at East Ship Island and Horn Island. These maxima correspond in depth to sandy and/or bedded zones evident in X-radiographs and profiles of sand concentration (see Figs. 4 and

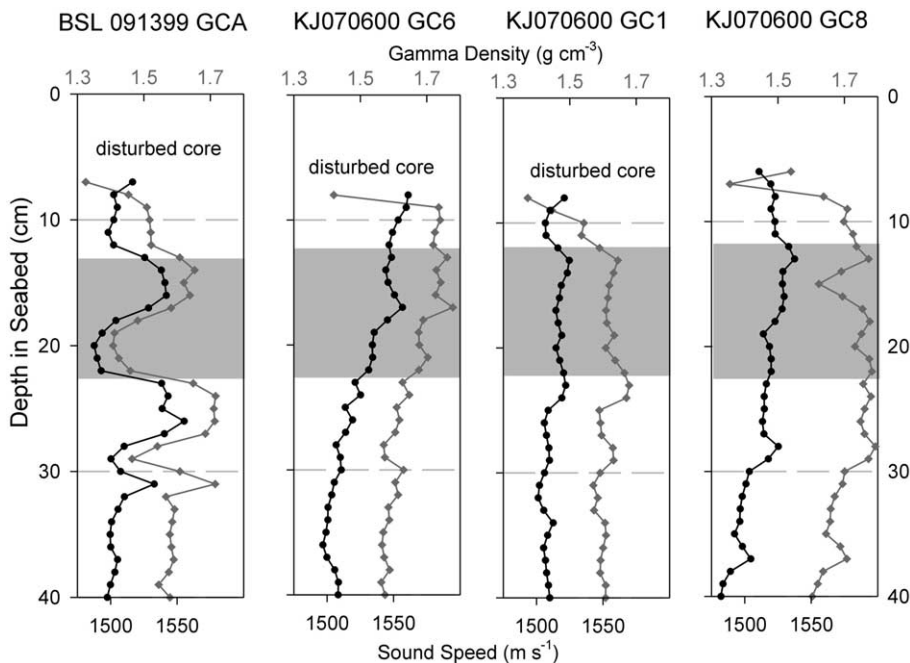


Fig. 6. Profiles of gamma density (g cm^{-3}) (circles) and compressional wave speed (m s^{-1}) (diamonds) from gravity cores. The shaded area indicates the disturbed ^{210}Pb profile (upper boundary) and penetration depth of ^{137}Cs (lower boundary).

5). This indicates that maximum values of both sound speed and gamma density are associated with elevated sand content in a regional bed. Shaded regions in Fig. 6 mark the depth of disturbed and/or vertical $^{210}\text{Pb}_{\text{xs}}$ profiles (upper boundary of shaded area) and maximum penetration depths of ^{137}Cs (lower boundary of shaded area).

4.5. Interpretation of sedimentological and radiochemical observations

Cores collected from Mississippi Sound and the adjacent inner shelf (from an area $>300\text{ km}^2$) display a regional layer of sediment below $\sim 12\text{ cm}$ bsf that is characterized by elevated sand content (Figs. 4–6), localized stratification at comparable depths bsf (Fig. 4, cores KJ 070999 BCE and KJ070600 BC8), and low and vertically uniform $^{210}\text{Pb}_{\text{xs}}$ activity (Fig. 3). This layer also contains the deepest detectable ^{137}Cs (Fig. 3), implying that some of the particles within it were deposited after 1954 and probably after 1963 as well. A recent small-scale study of these same sandy beds in western Mississippi Sound (Bentley et al., 2000) indicates that there is significant variability in bed thickness (1–10 cm) and preservation (faintly to intensely bioturbated) at spatial scales $<1\text{ km}$, however, small scale patterns are generally consistent with regional trends identified here. Because similarities in this study are observed in cores collected across a wide region, we suggest that the most plausible process for producing a regional bed like the one discussed in this study is a single intense regional sediment resuspension and transportation event, and we propose that the most likely candidate is Hurricane Camille in 1969.

There are other possible causes of such a widespread sandy layer in nearshore waters, i.e. a river flood event (Geyer et al., 2000; Huh et al., 2001), spoil dumping from channel dredging operations (Morton et al., 2001), local resuspension during cold fronts (Walker and Hammack, 2000), and regional resuspension and transport during tropical cyclones (Walker, 2001). It is also possible that such a widespread bed could result from multiple causes, such as the effects of several tropical

cyclones or a number of years with severe winter storms. Multiple causes should produce irregular sandy layers as seen in the cores but they would not produce uniform mixing as indicated by the radiometric data, which argue for a single, large, intense event. Furthermore, the lack of significant event–layer formation by Hurricane Georges in 1998 (S.J. Bentley, unpublished data), suggests that these sandy layers are unique.

The most intense sediment transport in the northern Gulf of Mexico occurs during hurricanes (Stone et al., 1997). The strongest hurricane in the northern Gulf of Mexico in the twentieth century was Hurricane Camille, which made landfall in 1969 near the location where most of the cores for this study were collected (Fig. 1). The only other major hurricanes to impact this coastline during the past century were an unnamed category four hurricane, which made landfall at Pass Christian in 1947 (Neumann, 1993), and Hurricane Elena, which made landfall near Biloxi, MS, in 1985. The 1947 storm predates the 1954 release of ^{137}Cs and, consequently, cannot have produced the event layer we have identified. Hurricane Elena's impact on the seabed (1985) was not documented, however, surge and wind data (Stone et al., 1997) suggest that Elena's effects were comparable to those of the weaker Hurricane Georges. It is therefore probable that this regional bed resulted from widespread sediment remobilization, mixing, and deposition during Hurricane Camille.

The Camille event bed would have been generated in two stages (Aigner and Reineck, 1982, Snedden and Nummedal, 1990). First, a sandy basal layer was produced by resuspension, erosion, advection, and deposition of coarse sediment. Second, a mud drape was deposited after the storm peak. This secondary sedimentation also includes both coarse and fine sediment from river runoff associated with storm rainfall.

Radiochemical and fabric analyses suggest that the initial thickness of the Camille layer at Bay St. Louis (core KJ070999 BCE in Figs. 1 and 4) was 10–15 cm (Bentley et al., 2000). This bed consists of a sandy basal layer approximately 5 cm thick and an overlying mud drape 5–10 cm thick. Subsequent disruption by bioturbation destroyed pri-

mary bedding in the upper 5–10 cm (the mud drape) of the Camille layer at that location. The basal sandy layer is also truncated and only discontinuous sandy lenses with faint internal lamination in a bioturbated muddy matrix are preserved.

The cores collected near Horn and Ship Islands and the adjacent inner shelf (Fig. 1) cannot be used to constrain the original sandy layer thickness but they do indicate a total bed thickness similar to that at Bay St. Louis. It is probable that the storm layer at these locations would have contained more sand because of the higher sand content near the barrier islands (see Fig. 2). However, fabric evidence (Fig. 4) shows that post-depositional bioturbation has destroyed most primary stratification in the central part of Mississippi Sound. A zone of bioturbated sandy mud is sandwiched between zones of bioturbated muddy sand in these cores. For these cores, the best evidence for initial bed geometry comes from $^{210}\text{Pb}_{\text{xs}}$ and ^{137}Cs data.

Before the impact of Camille in 1969, the penetration depth of ^{137}Cs into the seafloor would probably have been on the order of 5–10 cm, transported into the seabed primarily by bioturbation (e.g. Nittrouer et al., 1984). If this thickness of sediment was reworked and redeposited as the Camille event bed, all sediment in the seabed that was labeled with ^{137}Cs would have been reworked. The penetration depth of ^{137}Cs would then become a marker for the base of the Camille bed, a marker that could be preserved if it was buried deep enough to escape further vertical mixing of sediment.

Observations of sedimentary fabric indicate that deep bioturbation does occur (Fig. 4), but biogenic particle mixing does not appear to have produced significant downward mixing of particles and ^{137}Cs below the uppermost 5–10 cm of the seabed. This is revealed in the $^{210}\text{Pb}_{\text{xs}}$ profiles (Fig. 3) at Horn Island (core KJ070600 BC1), East Ship Island (core KJ070600 BC6), and on the inner shelf (core KJ070600 BC8). They preserve sharp $^{210}\text{Pb}_{\text{xs}}$ discontinuities at approximately 12 cm bsf, which would have been destroyed if significant post-depositional vertical mixing had occurred over spatial scales $> \sim 2$

cm. It is also important to note that this depth is not marked by an abrupt vertical change in grain size, which could also produce this discontinuity. Instead, the dominant mode of bioturbation below ~ 10 cm in the seabed appears to have been local and horizontal mixing (e.g. Wheatcroft et al., 1990), which is capable of destroying primary depositional fabric over spatial scales of mm without significantly altering profiles of particle-bound radionuclides that are sampled at spatial scales of cm. Thus, the Camille bed contains a preserved radiochemical signature that is characterized by an upper boundary marked by a discontinuity in the $^{210}\text{Pb}_{\text{xs}}$ profile, a lower boundary marked by the maximum depth of ^{137}Cs , and relatively constant $^{210}\text{Pb}_{\text{xs}}$ activities throughout. Using these criteria, the initial thickness of the bed in cores we have analyzed was at least 10 cm at a depth of approximately 12–22 cm bsf (Figs. 3 and 4), including both the mud drape and basal sandy zone. Cores shown in Figs. 3–6 were collected from the sand-mud transition in shelf and sound settings, in order to maximize lithologic contrast between event beds and ‘fair-weather’ sediments (facilitating recognition of bed boundaries), and to allow application of $^{210}\text{Pb}_{\text{xs}}$ and ^{137}Cs geochronology (which requires fine-grained sediments). As a result, bed parameters derived from these cores typify only a small portion of the study area, over which the Camille bed probably displayed considerable variability both in initial thickness and lithology. Because of the likely post-depositional destruction of beds thinner than ~ 10 cm, and difficulties associated with sampling and analyzing thicker event layers in hard, sandy substrate, numerical modeling provides an excellent means to explore initial bed characteristics over a wide region.

5. Numerical modeling results

The numerical sedimentation model TRANS98 is used in this study to identify probable relationships between the physical forcing during Hurricane Camille and the resulting event bed in Mississippi Sound and the nearby shelf. To achieve this goal, we will examine the most direct forcing

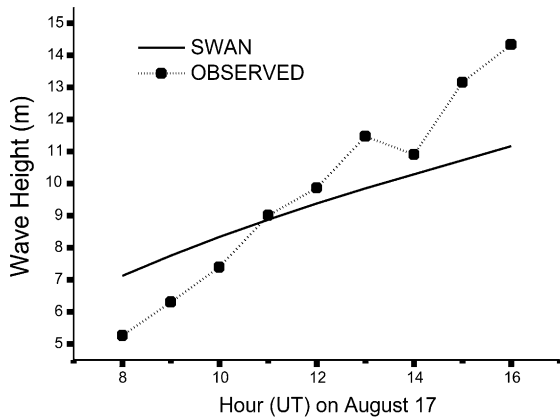


Fig. 7. Time series of significant wave heights measured at an offshore oil platform 50 km east of the Mississippi River delta front (squares) and predicted by the SWAN model.

fields for storm bed generation, the waves and currents. These will then be compared to the resulting event layer predicted by TRANS98.

5.1. Modeled wave and current fields

The eye of Hurricane Camille passed over the modern Mississippi River delta within 23 km of an oil platform (South Pass 62A), which was located 100 km south of Mississippi Sound in a water depth of 100 m. The observed deep-water significant wave heights, indicated by squares in Fig. 7, were greater than 10 m as the storm passed on August 17 (Patterson, 1976). The SWAN model predicts similar wave heights at mid-day but they do not increase as rapidly as the observations. Although the modeled H_s is 20% lower than observed at 16.00 h UT, this comparison shows that the simple wind model produces reasonable wind fields and the resulting waves are adequate for this application.

Hurricane Camille produced a storm surge of more than 7 m along the landward margin of Mississippi Sound (Thom and Marshall, 1971), which is capable of overtopping all of the barrier islands. The ADCIRC model predicts a maximum storm surge of 10.6 m at 06.00 h UT on August 18. The storm waves inside the lagoon would thus have been significantly larger than for most conditions. SWAN uses the predicted storm surge to

calculate the storm waves. Consequently, the predicted waves are also much larger within the estuary. Despite the increased water depths within the sounds, the shallow continental shelf within the Mississippi Bight significantly limits wave generation and attenuates waves propagating from deep water, and results in much lower waves within the study area. Thus, the predicted wave heights (Fig. 8A) at the storm maximum (03.00 h UT on August 18) are only 3 m on the Gulf side of the barriers and between East Ship Island and Horn Island. Predicted wave heights within Mississippi Sound are greater than 1.5 m. The storm waves remain large after the storm surge peaks (Fig. 8B), as the storm surge begins to ebb from within the sound.

The storm bottom currents (Fig. 9A), predicted by ADCIRC, flow into Mississippi Sound through the wide inlet between East Ship Island and Horn Island as the storm surge is increasing. This flow pattern persists for less than 6 h but the maximum velocity is almost 2 m s^{-1} . The modeled currents do not include overtopping of the barrier islands, but the predicted bottom currents reproduce realistic topographic steering around the islands. The flow is almost directly northward at this time on the Gulf side of the islands. After the storm surge peak, the flow reverses direction (Fig. 9B) and currents as strong as the flood tide flow offshore over the islands and through the passes during the next 7 h. Note that the ebb flow is eastward on the Gulf side of the islands rather than southward. Thus, the flood and ebb flows are not symmetrical. This suggests that net deposition should be more prevalent seaward of the islands.

5.2. Model-predicted storm sedimentation

Combined wave and current action resuspends bottom sediments repeatedly, but if currents to transport this sediment are lacking, it will be re-deposited with no net change in bed height. This is a common situation on the continental shelf where weak bottom flows coincide with long-period swell (Lentz and Trowbridge, 1991). Strong flows are more common in shallow water near the coast, with the strongest bottom currents oc-

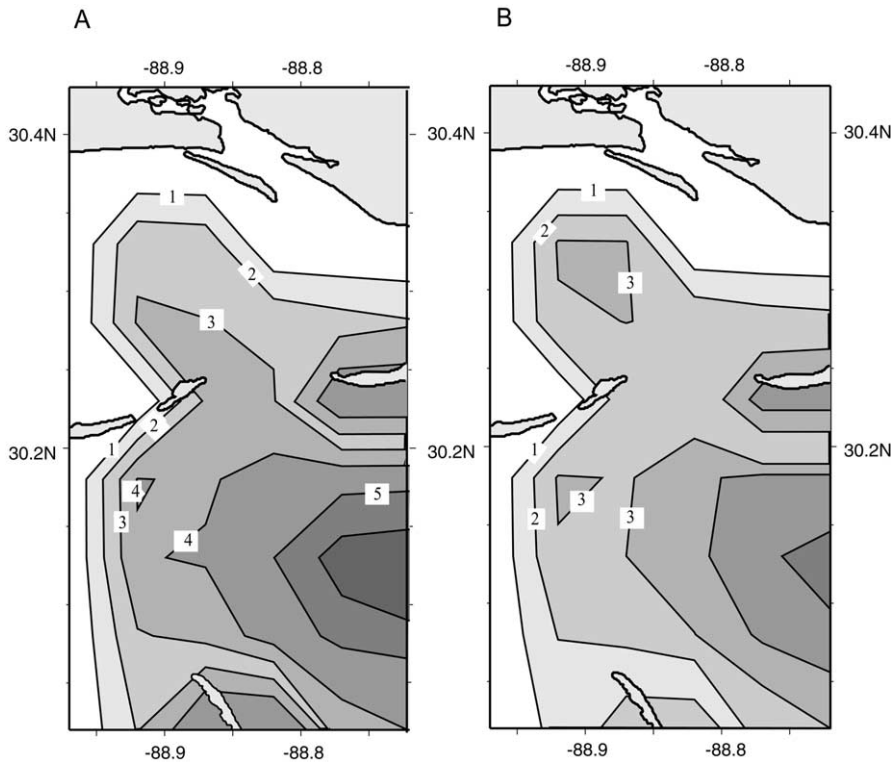


Fig. 8. Contour plots of significant wave height calculated by the SWAN wave model at (A) 0300 UT and (B) 0900 UT on 18 August. Contour interval is 0.5 m.

curing during hurricanes and other severe storms. Because of rapidly changing bottom flow during hurricanes, it is expected that sediment transport pathways will be highly variable as well. Unsteady flows will produce irregular storm beds as have been predicted for tropical cyclones on the Texas shelf (Keen and Slingerland, 1993a,b). The total storm bed, which would be observed in both cores and outcrops, can be defined as the sum of resuspension and deposition (Keen and Glenn, 1998). The numerical sedimentation model can differentiate these processes and show their relationship to the final storm bed.

The finite-difference formulation for bed conservation used in TRANS98 computes erosion, and the resulting decrease in bed elevation, for a net flux of sediment out of a model grid point. A map of the cumulative erosion depth during Hurricane Camille (Fig. 10) indicates the complexity of the sediment transport field during the storm.

The irregular erosive surface is an indication of the rapidly changing flow field during the storm surge buildup and ebb stages. Maximum erosion exceeds 160 cm at several locations on the sound side of the islands. These maximum erosion depths are herein considered as qualitative indicators of extensive beach and dune erosion by overwash of the barriers. Erosion is also significant in the channel immediately west of Horn Island. Average depths of erosion are about 10 cm between the islands and on the shelf to the southeast, and slightly less to the southwest.

Sediment is continuously resuspended by wave and current action. Thus, resuspension is common even in a transport-dominated storm regime. Because resuspension is a rapid process compared to advection, reworking extends below the erosion depth caused by transport. Resuspension depths predicted by TRANS98 (Fig. 11) are more than 3 cm on the seaward side of the barriers and in-

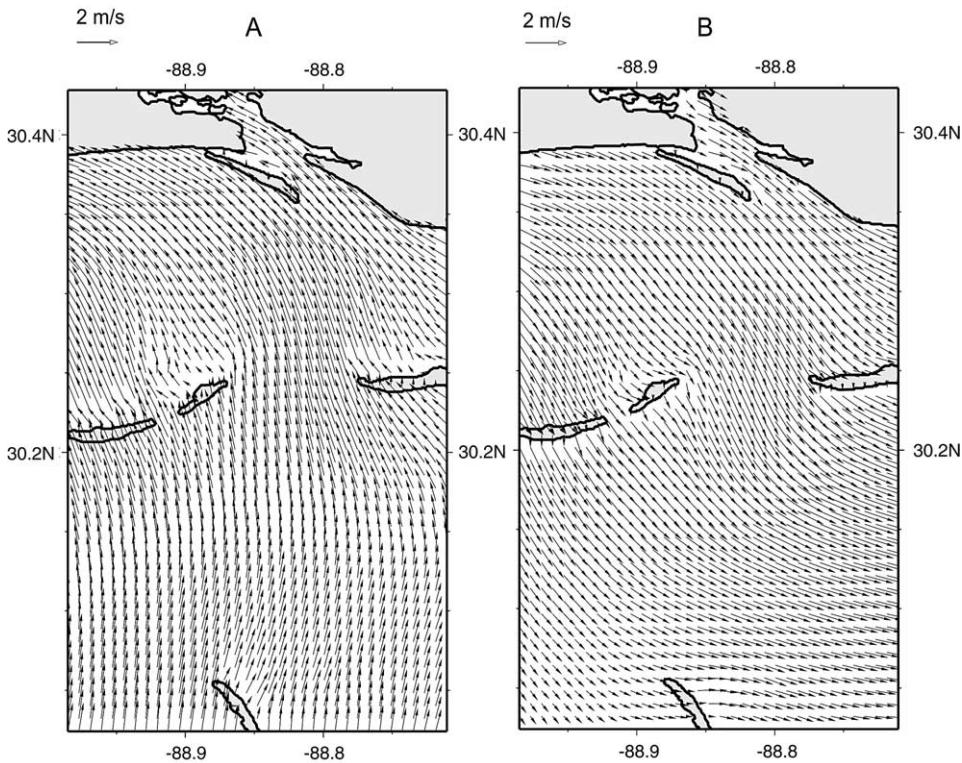


Fig. 9. Vector plots of the depth-averaged currents calculated by ADCIRC in Mississippi Sound at (A) 0300 UT and (B) 0900 UT on 18 August.

crease in deeper water towards the open sea. On the landward side of the islands, where the cores were collected (see Fig. 1), resuspension is reduced because the sedimentation regime is dominated by erosion and deposition. Resuspension depths are about 2 cm inside the sound.

The final storm bed (Fig. 12) consists of both transported and resuspended sediment. This storm bed is highly irregular in plan view. Its local thickness exceeds 300 cm near the barrier islands but the greatest deposition is predicted along the Gulf side of Horn Island. This sediment originated from the island during flooding of the estuary (Fig. 9A). The transport paths are short, however, because of the rapid change in the current direction; predicted currents exceed 1 m s^{-1} for only 5 h. Consequently, this sediment is deposited in the areas indicated by more than 68 cm in Fig. 12. The physical interpretation of these deposits is that the barrier islands were breached,

with channels incised to the lagoon, and sediment was subsequently deposited as overwash fans while flow was into the sound. This process did in fact occur during Hurricane Camille; the narrow channel between East Ship Island and West Ship Island was named Camille Breach after its mode of formation. It is not possible to predict exactly where breaching would have occurred, however, even if wetting and drying processes were included in both the current and sedimentation models. Large thicknesses of sand on the seaward sides of the islands were deposited during the ebb flow (Fig. 9B), which exceeded 1 m s^{-1} for 6 h. Thus, barrier island sand was deposited as storm surge ebb deltas greater than 68 cm in thickness, and linear sheets varying from 10 to 50 cm on the inner shelf south of the islands. Because of the difficulty of constraining the volume of sediment eroded from the islands, it is possible that these predicted inner shelf beds are

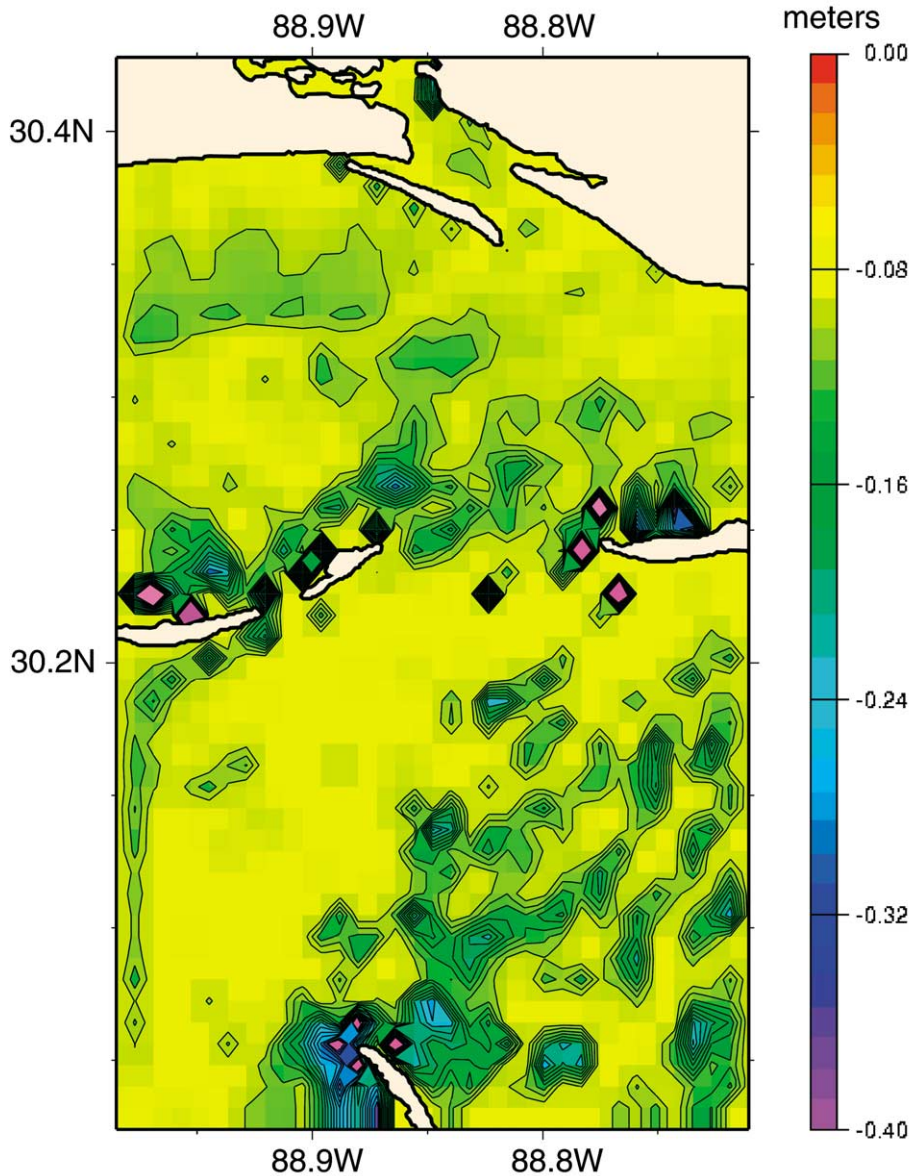


Fig. 10. Cumulative erosion depth computed by TRANS98 for Hurricane Camille. Values deeper than -0.4 m are shown in purple.

too thick. The storm bed varies from 10 to 30 cm in the pass between East Ship Island and Horn Island.

A simulated cross-section across the pass between East Ship Island and Horn Island (Fig. 13) summarizes the net storm deposition in the area. The erosion depth varies from -19 cm at Ship

Island (station 2) to -10 cm at Horn Island (station 4). Erosion is significantly less on the open shelf (station 1) because transporting currents were greatest during the ebb surge when the sediment-laden flow was seaward. Modeled resuspension is uniform across the pass because large waves in this area coincided with strong currents,

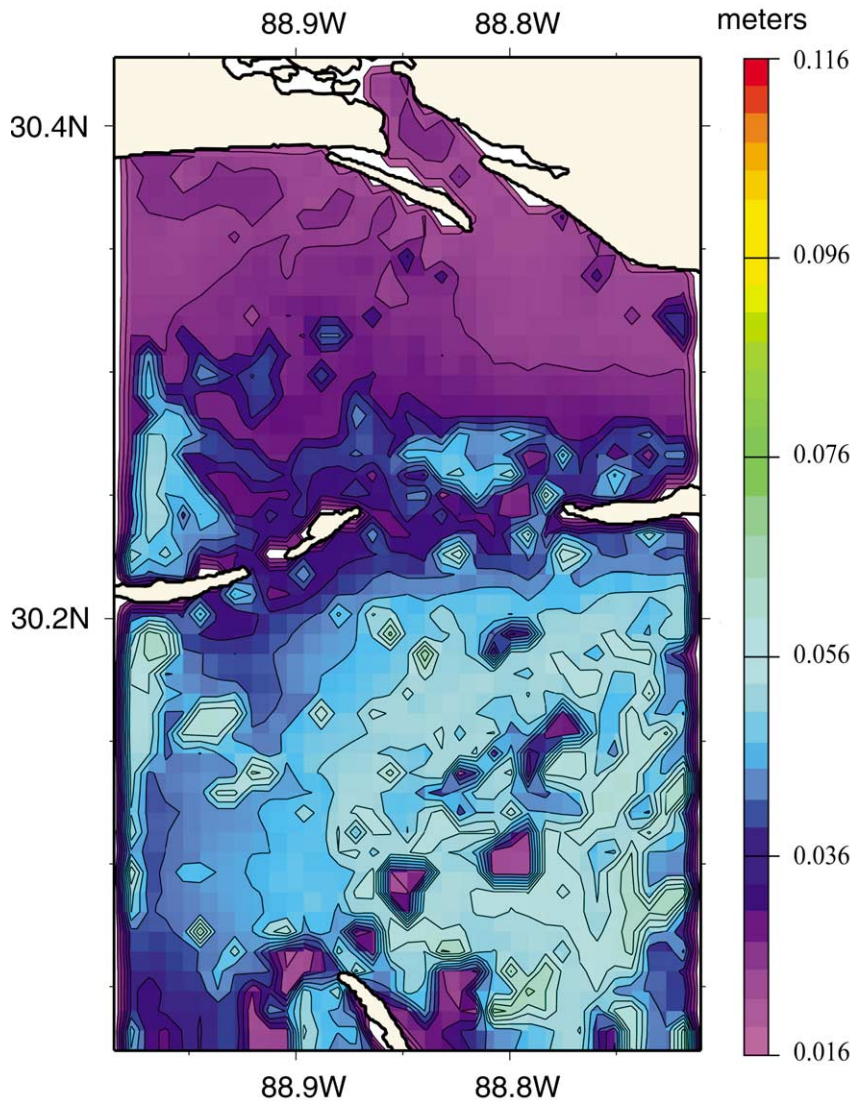


Fig. 11. Cumulative thickness of resuspended sediment computed by TRANS98 for Hurricane Camille.

which persisted until the very end of the storm when wave action was significantly reduced. This is why the resuspension contribution to the storm bed is less than 4 cm. The most dramatic contribution to the storm bed is deposition from currents. Deposition at East Ship Island has increased the bed elevation by more than 20 cm, whereas local erosion from the sound side of Horn Island increases the bed height by more than 40 cm at station 4. Significant quantities of barrier island sand were deposited on the inner

shelf, producing a net increase of more than 20 cm in bed elevation.

6. Discussion

6.1. Origin of the storm layer

The storm bed deposited by Hurricane Camille initially consisted of both coarse and fine sediment. Sandy sediment was resuspended and de-

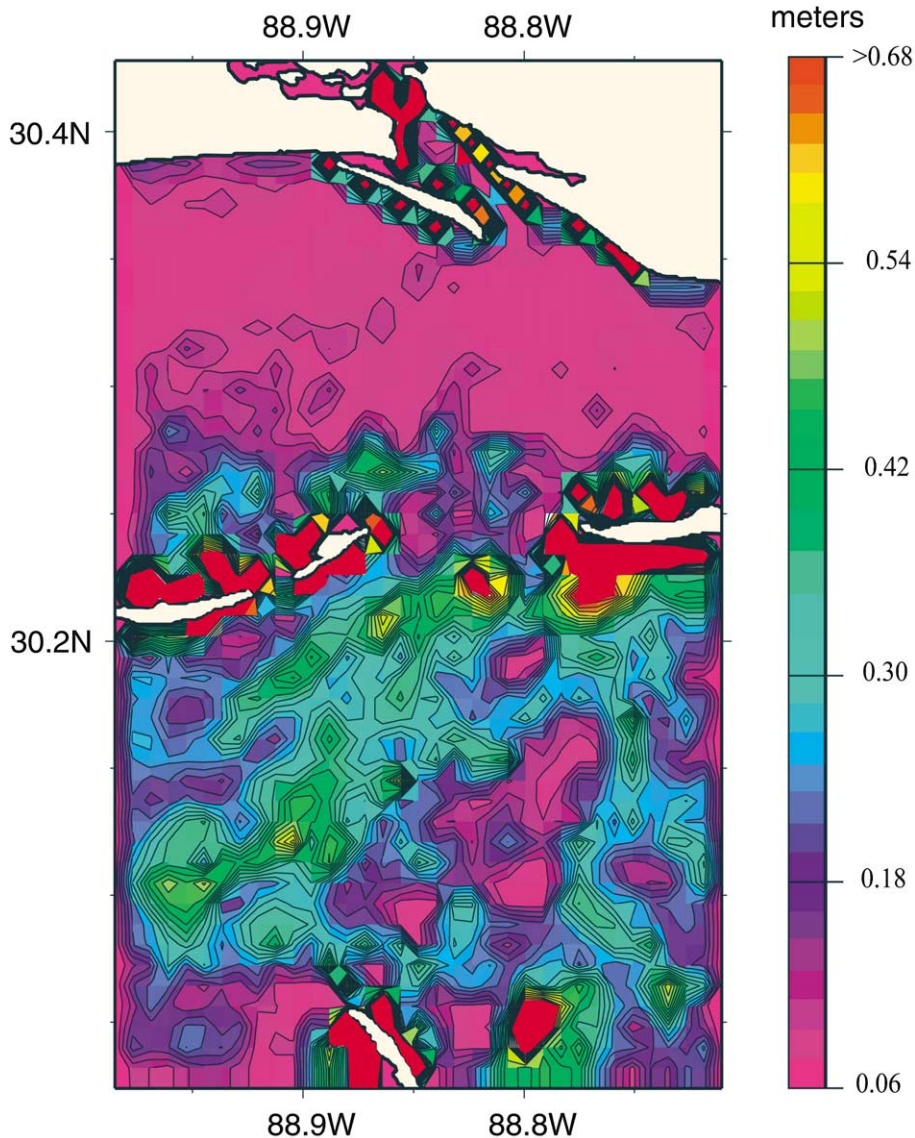


Fig. 12. Final storm sand layer thickness computed by TRANS98 for Hurricane Camille. Values thicker than 0.62 m are shown in purple.

posited as a discrete layer whereas the fine sediment was deposited as a drape after the turbulence had decreased. Post-storm terrestrial runoff would have deposited mixed sediment within the estuary, especially near river mouths. The bottom of the sand layer can be most easily identified in cores by its erosive base. This study has used radiometric methods to identify the possible top of the storm bed in several cores. These methods are

sensitive to bioturbation and physical mixing, but it is reasonable to assume that a bed with an initial thickness greater than 6 cm would be identifiable by radiometric methods today if no subsequent large storms occurred.

Combined oscillatory and steady currents act to entrain both fine and coarse sediment from the bed. The settling velocities of the coarse sediment are on the order of 1 cm s^{-1} whereas clay flocs

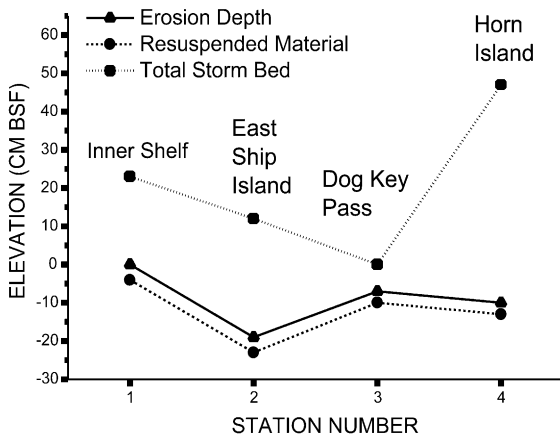


Fig. 13. Cross-section of erosion (triangles), resuspension (circles), and deposition (squares) across the pass between East Ship Island and Horn Island. The figure also includes the offshore station (No. 1). The numbers refer to locations on Fig. 1.

have settling velocities on the order of 0.01 cm s^{-1} (Burban et al., 1990). Consequently, the sand layer can be modeled independently of the clay as a first approximation. A fundamental assumption of this approach is that all sediment will be entrained by the storm waves. We assume that the critical shear stress for the cohesive sediments will be exceeded by the storm waves. Nevertheless, the flow will reach its sediment load limit after a few cm of sand have been suspended from the bed. This mechanism sorts the sediment out into a near-bed coarse fraction and a fine fraction distributed throughout the water column. The coarse sediment settles within minutes after the bottom shear stress decreases below the sediment critical entrainment threshold. Because of the sensitivity of deposition to bottom stress, it is expected that the sand layer will be highly variable laterally.

From core analysis, the Camille sand layer is estimated to be on the order of 5 cm thick at Bay St. Louis, which is similar to the values predicted inside the sound by the model (Fig. 12). The initial thickness is more difficult to estimate from the cores near the barrier islands. The model predicts a sand layer 5–30 cm thick near both Ship Island and Horn Island, not counting local beds associated with barrier erosion. The total modeled sand

layer is less than 30 cm thick between the islands where intense wave and current action would have transported sediment through the pass during the storm. This area is thus likely to consist of homogeneous sand that is reworked by even moderate storms. The moderate ($< 10 \text{ cm}$) erosion predicted by the model on the inner shelf (Fig. 10) implies that storm layers might accumulate in this area in light of moderate resuspension and significant deposition (Fig. 13). This is supported by our analyses of the inner shelf box core (KJ070600 BC8), which contains clear stratification and erosive bases to sandy layers.

Caution must be used in comparing the storm bed thickness predicted by the model to the cores, because of fundamental differences between the measurement techniques and the modeling approach. For example, the initial thickness of the sand layer cannot be measured in the cores whereas the model predicts this thickness only. Furthermore, the cores sample the storm bed sparsely and do not accurately represent the bed's lateral variability; thus, it is not possible to determine if the large spatial variability seen in the modeled bed is correct. Other factors that must be considered in making direct comparisons are the effect of the model grid resolution, landward boundary conditions, and uncertainties in the predicted waves and currents. As seen in the modeled wave and current fields, Mississippi Sound and the adjacent shelf were subjected to strong and variable forcing, which is difficult to reproduce with the numerical models without observations. The model predicts sandy beds that may be as much as an order of magnitude too thick near the islands and on the shelf, which is partly attributable to the uncertainties in forcing, the use of a single sediment distribution, and the neglect of cohesive sediment effects.

6.2. Preservation of the Camille Bed

The sandy layer observed in the cores is on the order of 10 cm thick. The storm bed predicted by the sedimentation model has a similar thickness in the vicinity of the core locations. Rapid bioturbation in the study area is restricted to depths of $< 5\text{--}7 \text{ cm bsf}$ (Bentley et al., 2000). This suggests

that the upper 5–7 cm of the Camille storm bed would have been modified significantly by bioturbation, whereas the basal portion could escape biogenic destruction. This appears to be the case in X-radiographs of cores from the inner shelf (KJ070600 BC8) and Bay St. Louis (KJ070999 BCE) (Fig. 4). Clearly, there has also been significant biogenic modification of fabric for basal portions of the storm bed in cores from Horn and Ship Islands, but by deeper, slower bioturbation than described above. Nevertheless, grain size and radioisotopic signatures persist (Figs. 3–6).

With respect to physical destruction of the storm bed, both hurricanes and winter cold fronts produce sediment transport in the study area. The other hurricanes to pass over this region since 1969 were the much weaker hurricanes Georges (1998) and Elena (1985), which made landfall 50 km east of Camille's landfall. More frequent processes associated with cold fronts can also produce erosion and deposition on the shoreface of the barrier islands (Stone and Wang, 1999). As noted by Kahn and Roberts (1982), the shoreface deposits generated by a hurricane can be redistributed at the annual time scale. Thus, it is unlikely that the model-predicted beds near the shoreface of Horn Island would be preserved. It is also unlikely that any bed deposited within the channel west of Horn Island would be preserved. However, radiometric data from the cores in this study suggest that the original bed thickness can be estimated from radionuclide profiles. Furthermore, preservation of a significant fraction of the original storm bed has occurred at seafloor depths below the sand-to-mud transition, which is approximately 5 m in Mississippi Sound and 10 m on the inner shelf.

6.3. Regional sedimentation rates

Model-predicted increases in bed elevation (due to advection of sand) and probable net deposition associated with the post-storm mud drape imply that net deposition from Camille made a significant contribution to the long-term accumulation rate in Mississippi Sound and the adjacent inner shelf. Ludwick (1964) calculated an accumulation rate of 24 cm ky^{-1} for the Holocene sediments of

Mississippi Sound. This is an order of magnitude smaller than the maximum $^{210}\text{Pb}_{\text{xs}}$ accumulation estimated for the cores from East Ship Island and Horn Island (0.29–0.47 cm y^{-1} averaged over the past 50 yr; Fig. 3, Table 2). The large difference between data in Table 2 and Ludwick's estimates for the Holocene are not surprising, considering the combined effects of time-averaging (decreasing rate with longer averaging period) and hurricane-induced sedimentation. Sediment dynamics produced by hurricanes and other intense physical processes can steepen $^{210}\text{Pb}_{\text{xs}}$ profiles by both reworking existing sediment (Dellapenna et al., 1998), and by introducing new sediment, meaning that apparent rates in Table 2 are likely to overestimate actual sedimentation rates on decadal timescales. Nevertheless, if major hurricanes such as Camille have return periods of more than 100 yr and can result in net sediment deposition on the order of 10 cm, then hurricane-associated deposition could have produced the total thickness of Holocene deposits in Mississippi Sound (1–4 m; Ludwick, 1964). Clearly, just as there is significant regional variability in the storm bed, there must be major differences in sediment transport produced by different storms. Nevertheless, hurricane-associated sediment transport is probably a major factor in long-term sediment accumulation.

7. Conclusions

A sandy layer has been identified in box cores and gravity cores throughout the Mississippi Sound region using fabric, radiochemical, and sedimentological methods. Based on these results, we attribute this sandy layer to Hurricane Camille, which made landfall on August 17, 1969. It is proposed that this event bed escaped total destruction by biological and physical mixing because of its thickness, which was on the order of 10 cm, and the lack of major hurricane landfalls in the area since its deposition.

The deposition of the original sandy storm bed by Hurricane Camille has been simulated using a numerical sediment resuspension and transport model. The model predicts a sandy bed that

ranges from less than 1 cm within the estuary to more than 160 cm near barrier islands. The bed is generated by both resuspension and transport processes. The major source of transported sediment is the shoreface on both the sound and Gulf sides of the islands. Resuspension produces a regional sand bed of 1–4 cm thickness. Local advection produces a highly variable sand layer. The predicted sand bed is consistent with the storm layer inferred from the cores.

The long-term sediment accumulation rate is sensitive to local advection during the storm, which can lead to low estimates in sediment source areas and high estimates in sink areas. Physical and biological processes are very important to the post-depositional modification of a storm layer. Consequently, because of non-uniform resuspension, erosion, deposition, and post-depositional modification by physical and biological processes, the preserved storm bed is not uniform in composition, thickness, or fabric.

Acknowledgements

S.J.B. was supported by the Office of Naval Research Grant N00014-00-1-0768 and Naval Research Laboratory Grant N00173-00-1-G907. T.R.K. was supported by the Office of Naval Research Program element 0601153N. C.A.B. was supported by the Office of Naval Research Program element 0602435N. The authors also thank the captain and crew of the R/V *Kit Jones* for field assistance. We thank Yoko Furukawa and Dawn Lavoie for ship-time support, and Will Vienne, Brian Velardo, and Bill Sawyer for data processing and core analyses. We also thank Mike Richardson and two anonymous reviewers for their valuable comments on earlier versions of this manuscript. Modeling and data requirements in support of the Northern Gulf of Mexico Littoral Initiative Project of the Naval Oceanographic Office motivated this study.

References

Aigner, T., Reineck, H.-E., 1982. Proximality trends in modern

- storm sands from the Helgoland Bight and their implications for basin analysis. *Senckenb. Mar.* 14, 183–215.
- Benninger, L.K., Aller, R.C., Cochran, J.K., Turekian, K.K., 1979. Effects of sediment mixing on the ^{210}Pb chronology and trace metal distribution in a Long Island Sound sediment core. *Earth Planet. Sci. Lett.* 43, 241–259.
- Bentley, S.J., Nittrouer, C.A., 1999. Physical and biological influences on the formation of sedimentary fabric in an oxygen-restricted depositional environment: Eckernförde Bay, southwestern Baltic Sea. *Palaios* 14, 585–600.
- Bentley, S.J., Furukawa, Y., Vaughan, W.C., 2000. Record of event sedimentation in Mississippi Sound. *Trans. Gulf Coast Assoc. Geol. Soc.*, 715–723.
- Blain, C.A., 1997. Modeling methodologies for the prediction of hurricane storm surge. In: Saxena, N. (Ed.), *Recent Advances in Marine Science and Technology*, 96. Pacon International, Honolulu, HI, pp. 177–189.
- Booij, N., Ris, R.C., Holthuijsen, L.H., 1999. A third generation wave model for coastal regions: 1. Model description and validation. *J. Geophys. Res.* 104, 7649–7666.
- Brenchley, P.J., 1985. Storm influenced sandstone beds. *Mar. Geol.* 9, 369–396.
- Brenchley, P.J., Romano, M., Gutierrez Marco, J.C., 1986. Proximal and distal hummocky cross-stratified facies on a wide Ordovician shelf in Iberia. In: Knight, R.J., McLean, J.R. (Eds.), *Shelf Sands and Sandstones*. Can. Soc. Pet. Geol. Mem. No. 11, pp. 241–256.
- Burban, P.Y., Xu, Y.J., McNeil, J., Lick, W., 1990. The flocculation of fine-grained sediments in estuarine waters. *J. Geophys. Res.* 95, 8323–8330.
- Cochran, J.K., 1982. The oceanic chemistry of the U- and Th-series nuclides. In: Ivanovich M., Harmon, R.S. (Eds.), *Uranium Series Disequilibrium: Applications to Environmental Problems*. Clarendon Press, Oxford, pp. 384–431.
- Cutshall, N.H., Larsen, I.L., Olsen, C.R., 1983. Direct analysis of ^{210}Pb in sediment samples: Self absorption corrections. *Nucl. Instrum. Methods* 206, 1–20.
- Dellapenna, T.M., Kuehl, S.A., Schaffner, L.C., 1998. Sea-bed mixing and particle residence times in biologically and physically dominated estuarine systems: a comparison of lower Chesapeake Bay and the York River subestuary. *Estuar. Coast. Shelf Sci.* 46, 777–795.
- Dott, R.H., Bourgeois, J., 1982. Hummocky stratification: Significance of its variable bedding sequences. *Geol. Soc. Am. Bull.* 93, 663–680.
- Duke, W.L., 1985. Hummocky cross-stratification, tropical hurricanes, and intense winter storms. *Sedimentology* 32, 167–194.
- Duke, W.L., Arnott, R.W.C., Cheel, R.J., 1991. Shelf sandstones and hummocky cross-stratification: New insights on a stormy debate. *Geology* 31, 171–190.
- Figueiredo, A.G., Jr., Sanders, J.E., Swift, D.J.P., 1982. Storm-graded layers on inner continental shelves: Examples from southern Brazil and the Atlantic coast of the central United States. *Sediment. Geol.* 31, 171–190.
- Flaum, J.A., Keen, T.R., Bartek, L.R., 2000. Modeling the stratigraphy that evolves in the transgressive systems tract

- of continental shelf margins with high sediment input and frequent intense storms, Geological Society of America Summit 2000 meeting, Reno, Nevada. Abstracts with Program 32(7), A-513.
- Gagan, M.K., Chivas, A.R., Herczag, A.L., 1990. Shelf-wide erosion, deposition, and suspended sediment transport during Cyclone Winifred, central Great Barrier Reef, Australia. *J. Sediment. Petrol.* 60, 456–470.
- Geyer, W.R., Hill, P., Milligan, T., 2000. The structure of the Eel River plume during floods. *Cont. Shelf Res.* 20, 2067–2093.
- Glenn, S.M., Grant, W.D., 1987. A suspended sediment correction for combined wave and current flows. *J. Geophys. Res.* 92, 8244–8246.
- Grant, W.D., Madsen, O.S., 1982. Moveable bed roughness in unsteady oscillatory flow. *J. Geophys. Res.* 87, 469–481.
- Hayes, M.O., 1967. Hurricanes as Geologic Agents: Case Studies of Hurricanes Carla, 1961, and Cindy, 1963. Report of Investigations No. 61. Bureau of Economic Geology, Texas University.
- Huh, O.K., Walker, N.D., Moeller, C., 2001. Sedimentation along the eastern Chenier Plain coast: Down drift impact of a delta complex shift. *J. Coast. Res.* 17, 72–81.
- Kahn, J.H., Roberts, H.H., 1982. Variations in storm response along a microtidal transgressive barrier-island arc. *Sediment. Geol.* 33, 129–146.
- Keen, T.R., Slingerland, R.L., 1993a. A numerical study of sediment transport and event bed genesis during Tropical Storm Delia. *J. Geophys. Res.* 98, 4775–4791.
- Keen, T.R., Slingerland, R.L., 1993b. Four storm-event beds and the tropical cyclones that produce them: a numerical hindcast. *J. Sediment. Petrol.* 63, 218–232.
- Keen, T.R., Glenn, S.M., 1994a. Coastal Circulation and Sedimentation during severe Storms. Proceedings of the 3rd International Conference on Estuarine and Coastal Modeling, pp. 279–293.
- Keen, T.R., Glenn, S.M., 1994b. A coupled hydrodynamic-bottom boundary layer model of Ekman flow on stratified continental shelves. *J. Phys. Oceanogr.* 24, 1732–1749.
- Keen, T.R., Glenn, S.M., 1998. Resuspension and advection of sediment during Hurricane Andrew on the Louisiana continental shelf. Proceedings of the 5th International Conference on Estuarine and Coastal Modeling, pp. 481–494.
- Keen, T.R., Stavn, R.H., 2000. Developing a capability to forecast coastal ocean optics: Minerogenic scattering. In: Spaulding, M.L., Butler, H.L. (Eds.), *Estuarine and Coastal Modeling VI*. American Society of Civil Engineers, Reston, VA, pp. 178–193.
- Lentz, S.J., Trowbridge, J.H., 1991. The bottom boundary layer over the northern California shelf. *J. Phys. Oceanogr.* 21, 1186–1201.
- Leutlich, R.A., Westerink, J.J., Scheffner, N.W., 1992. ADCIRC: An advanced three-dimensional circulation model for shelves, coasts, and estuaries. Report 1: Theory and Methodology of ADCIRC-2DDI and ADCIRC-3DI. Technical report DRP-92-6, Dept. of the Army, 168 pp.
- Ludwick, J.C., 1964. Sediments in Northeastern Gulf of Mexico. In: Miller, R.L. (Ed.), *Papers in Marine Geology: Shepard Commemorative Volume*. MacMillan, New York, pp. 204–238.
- Morton, R.A., 1981. Formation of storm deposits by wind-forced currents in the Gulf of Mexico and the North Sea. In: Nio, S.D., Shuttenehm, R.T.E., van Weering, T.C.E. (Eds.), *Holocene Marine Sedimentation in the North Sea Basin*. International Association of Sedimentologists, Special Publication No. 5, pp. 385–396.
- Morton, R.A., Nava, R.C., Arhelger, M., 2001. Factors controlling navigation-channel shoaling in Laguna Madra, Texas. *J. Waterw. Port Coast. Ocean Eng.* 127, 72–81.
- Murray, S.P., 1970. Bottom currents near the coast during Hurricane Camille. *J. Geophys. Res.* 75, 4579–4582.
- Nelson, C.H., 1982. Modern shallow-water graded sand layers from storm surges. Bering shelf: A mimic of Bouma sequences and turbidite systems. *J. Sediment. Petrol.* 52, 537–545.
- Neumann, C.J., 1993. *Tropical Cyclones of the North Atlantic Ocean, 1871–1977*. Washington, National Oceanic and Atmospheric Administration, 170 pp.
- Nittrouer, C.A., Sternberg, R.W., 1981. The formation of sedimentary strata in an allochthonous shelf environment: the Washington continental shelf. *Mar. Geol.* 42, 201–232.
- Nittrouer, C.A., DeMaster, D.J., Mckee, B.A., Cutshall, N.H., Larsen, N.H., 1984. The effect of sediment mixing on ²¹⁰Pb accumulation rates for the Washington continental shelf. *Mar. Geol.* 54, 201–221.
- Otvos, E.G., 1970. Development and migration of barrier islands, northern Gulf of Mexico. *Geol. Soc. Am. Bull.* 81, 241–246.
- Otvos, E.G., 1979. Barrier island evolution and history of migration, north central Gulf coast. In: Leatherman, S.P. (Ed.), *Barrier Islands from the Gulf of St. Lawrence to the Gulf of Mexico*, pp. 291–319.
- Patterson, M.M., 1976. Oceanographic data from Hurricane Camille. *J. Pet. Technol.* 28, 345–351.
- Ris, R.C., Holthuijsen, L.H., Booij, N., 1999. A third generation wave model for coastal regions: 2. Verification. *J. Geophys. Res.* 104, 7667–7681.
- Sawyer, W., 2001. Mean Phi Map of Surficial Bottom Sediments for Mississippi Sound and the La/MS Continental Shelf. <http://www.navy.mil/cgi-bin/graphic.pl/metoc/239/116/0-0-18/2, Draft 4/27/01>.
- Seilacher, A., 1982. General remarks about event deposits. In: Einsele, G., Seilacher, A. (Eds.), *Cyclic and Event Stratification*. Springer-Verlag, New York, pp. 161–174.
- Slingerland, R.L., Keen, T.R., 1999. Sediment transport in the Western Interior Seaway of North America: Predictions from a climate-ocean-sediment model. In: Bergman, K.M., Snedden, J.W. (Eds.), *Isolated Shallow Marine Sand Bodies: Sequence Stratigraphic Analysis and Sedimentologic Interpretation*. SEPM Special Publication No. 64, pp. 179–190.
- Snedden, J.W., Nummedal, D., 1990. Coherence of surf zone and shelf current flow on the Texas (U.S.A.) coastal margin: Implications for interpretation of paleo-current measurements in ancient coastal sequences. *Sediment. Geol.* 67, 221–236.

- Snedden, J.W., Nummedal, D., Amos, A.F., 1988. Storm- and fair-weather combined flow on the central Texas continental shelf. *J. Sediment. Petrol.* 58, 580–595.
- Stone, G.W., Stapor, F.W., 1996. A nearshore sediment transport model for the northeast Gulf of Mexico coast. *J. Coast. Res.* 12, 786–792.
- Stone, G.W., Wang, P., 1999. The importance of cyclogenesis on the short-term evolution of Gulf coast barriers. *Trans. Gulf Coast Assoc. Geol. Soc.* XLIX, 47–48.
- Stone, G.W., Grymes, J.W., Dingler, J.R., Pepper, D.A., 1997. Overview and significance of hurricanes on the Louisiana Coast, U.S.A.. *J. Coast. Res.* 134, 656–669.
- Stone, G.W., Wang, P., Pepper, D.A., Grymes, J.W., Roberts, H.H., Zhang, X.P., Hsu, S.A., Huh, O.K., 1999. Researchers begin to unravel the significance of Hurricanes of the northern Gulf of Mexico. *EOS, Transactions of the American Geophysical Union* (in press).
- Swift, D.J.P., Thorne, J.A., 1991. Sedimentation on continental margins, I: A general model for shelf sedimentation. In: Swift, D.J.P., Oertel, G.F., Tillman, R.W., Thorne, J.A. (Eds.), *Shelf Sand and Sandstone Bodies*. International Association of Sedimentologists, Special Publication No. 14. Blackwell Scientific, Boston, MA, pp. 3–32.
- Swift, D.J.P., Hudelson, P.M., Brenner, R.L., Thompson, P., 1987. Shelf construction in a foreland basin Storm beds, shelf sand bodies, and shelf-slope sequences in the Upper Cretaceous Mesaverde Group, Book Cliffs, Utah. *Sedimentology* 34, 423–457.
- Swift, D.J.P., Young, R.A., Clarke, T.L., Vincent, C.E., Niedoroda, A., Lesht, B., 1981. Sediment transport in the Middle Atlantic Bight of North America: Synopsis of recent observations. In: Nio, S.D., Shuttenehm, R.T.E., van Weering, T.C.E., *Holocene Marine Sedimentation in the North Sea Basin*. International Association of Sedimentologists, Special Publication No. 5, pp. 361–383.
- Thom, H.C.S., Marshall, R.D., 1971. Wind and surge damage due to Hurricane Camille. *J. Waterw. Harbors Coast. Eng. Div. Am. Soc. Civil Eng.* 97, 355–363.
- Thorne, J.A., Grace, E., Swift, D.J.P., Niedoroda, A., 1991. Sedimentation on continental margins, III: The depositional fabric-and analytical approach to stratification and facies identification. In: Swift, D.J.P., Oertel, G.F., Tillman, R.W., Thorne, J.A. (Eds.), *Shelf Sand and Sandstone Bodies*. International Association of Sedimentologists, Special Publication No. 14. Blackwell Scientific, Boston, MA, pp. 59–88.
- Upshaw, C.F., Creath, W.B., Brooks, F.L., 1966. Sediments and microfauna off the coasts of Mississippi and adjacent states. *Mississippi Geol. Surv. Bull.* 106, 127 pp.
- Walker, N.D., 2001. Tropical storm and hurricane wind effects on water level, salinity, and sediment transport in the river-influenced Atchafalaya-Vermillion Bay system, Louisiana, USA. *Estuaries* 24, 498–508.
- Walker, N.D., Hammack, A.B., 2000. Impacts of winter storms on circulation and sediment transport: Atchafalaya-Vermillion Bay region, Louisiana, USA. *J. Coast. Res.* 16, 996–1010.
- Walker, R.G., 1984. Shelf and shallow marine sands. In: Walker, R.G. (Ed.), *Facies Models*. Geological Association of Canada Reprint Series 1. Ainsworth, Kitchener, ON, pp. 141–170.
- Wheatcroft, R.A., Jumars, P.A., Smith, C.R., Nowell, A.R.M., 1990. A mechanistic view of the particulate biodiffusion coefficient: step lengths, rest periods, and transport directions. *J. Mar. Res.* 48, 177–207.